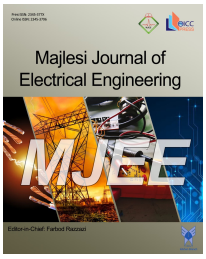

Volume 19, Issue 1, 192506 (1-11)

Majlesi Journal of Electrical Engineering (MJEE)

https://doi.org/10.57647/j.mjee.2025.1901.06

Nine switch converter as promising technology to improve efficiency of power electronic equipment

Pooya Parvizi[1], Alireza Mohammadi Amidi[2,5,*], Milad Jalilian[3,5], Mohammad Reza Zangeneh[4,5]

[1]*Department of Mechanical Engineering, University of Birmingham, Edgbaston, United Kingdom.*
[2]*Department of Electrical Engineering, Razi University, Kermanshah, Iran.*
[3]*Department of Physics, Faculty of Science, Lorestan University, Khorramabad, Iran.*
[4]*Department of Energy, Shahid Beheshti University, Tehran, Iran.*
[5]*Pooya Power Knowledge Enterprise, Tehran, Iran.*

[*]**Corresponding author:** alireza.moamidi@gmail.com

Original Research

Received:
02 December 2024
Revised:
28 January 2025
Accepted:
10 February 2025
Published online:
01 March 2025

Abstract:

Nine switch converters (NSCs) are power electronic devices that utilize nine power switches to convert electrical energy from one form to another. These converters are commonly used in various applications within the power industry. In fact, this type of converter is a multi-port power electronic device that consists of two three-phase terminals and a DC link, similar to the twelve-switch back-to-back (BTB) converter. However, it distinguishes itself by reducing the number of active switches by 25%. Nine switch converters offer several advantages over traditional converters. They can provide improved efficiency, reduced harmonic distortion and enhanced control capabilities. Additionally, they can handle higher power levels and operate at higher frequencies, making them suitable for a wide range of power industry applications. Furthermore, they are cost-effective, compact, and adaptable to higher power levels. By distributing voltage and current across fewer switches, the overall stress on individual components is reduced, which can enhance the lifespan and reliability of the converter. This paper summarizes the various utilizations of NSCs in modern power systems and briefly reviews the related challenges and future prospects.

Keywords: Nine switch converters; Efficient converters; Modern power systems; Power electronic devices

1. Introduction

The power electronic converter (PEC) technology plays a crucial role in integrating new low-carbon technologies by connecting two or more energy systems. Its initial purpose was to facilitate an interface between a source and a load, but as technology has advanced, it now allows energy to flow in both directions. This means that some power converters need to be able to operate in both directions [1–3]. In various applications, the output of the PEC can either be a regulated or adjustable magnitude of direct current or a constant or adjustable frequency of alternative current with an adjustable magnitude. The PEC's input and output sides are independent of each other and can be either single-phase or three-phase. Generally, power flows from the source side to the load side. However, some low-carbon technologies have unique exceptions, like a photovoltaic system connected to the utility grid via a PEC where the power flow is from the PVs, which is a DC input source, to the AC utility. In certain systems, the direction of power flow can be reversed, depending on the operating condition. The battery energy storage system is an example of such a condition [4, 5].
The power industry is constantly seeking innovative solutions to enhance power conversion efficiency, reduce component counts, and improve overall system performance. In this regard, nine switch converters (NSCs) have emerged as a promising technology that addresses these challenges [6, 7]. A typical nine-switch converter comprises nine power semiconductor switches that are used to control the transfer of power between the input and output sides of the converter [8]. These semiconductor switches can either be MOSFETs, IGBTs, or other types. The nine-switch converter typically has three-phase inputs, which are usually connected to a rectifier, and it also has three-phase outputs that are connected to the load. The converter has two stages: the first stage is a voltage source converter (VSC) that oper-

ates as a rectifier or an inverter depending on the direction of the power flow, while the second stage is a current source converter (CSC) that operates as a boost or a buck converter, depending on the voltage level required by the load [9, 10]. The control system of the nine-switch converter consists of a controller that generates the pulse-width modulation (PWM) signals for the semiconductor switches, and it also includes a feedback loop that monitors the converter's operating conditions, such as the output voltage and current. Additionally, the nine-switch converter may have additional components that include an inductor, a filter capacitor, and a DC-link capacitor, which help to smooth out the voltage and current waveforms. These components make the nine-switch converter a complex but versatile piece of power electronics equipment that is widely used in various industrial applications [11–13].

The nine-switch converter has several advantages over other converters. The nine-switch converter is highly flexible in terms of the direction of power flow, voltage regulation, and fault tolerance. The converter can operate as a rectifier or an inverter, depending on the direction of power flow, and it can regulate the output voltage at different levels using the CSC stage [14, 15]. Also, NSCs have higher efficiency compared to other converters because they use fewer components and have reduced switching losses. The VSC stage of such a converter uses fewer switches to control the power, resulting in reduced power losses due to switching. Furthermore, it is capable of reducing harmonics compared to other converters because it uses a high-frequency PWM scheme to minimize the harmonic content in the output waveform. This helps to attenuate the distortion and noise in the output waveform and enhances the overall performance of the converter [16–18].

In addition, power quality improvement via the utilization of NSCs is feasible. They can regulate the output voltage with high precision and mitigate voltage fluctuations. This way, the stability and reliability of the power system could be upgraded. Lower component costs can be achieved by using fewer components. This results in reduced manufacturing costs and makes the converter affordable for a wide range of industrial applications [19, 20]. The significant advantages of NSCs are listed in Fig. 1.

In electric transportation, these converters enhance power conversion efficiency and reduce the size and cost of power electronics systems, which are crucial for electric vehicles [21]. In electric machine control, they offer improved performance in motor drives by enabling better modulation techniques that lead to higher torque and capability [22, 23]. In renewable energy integration, nine switch converters facilitate the seamless connection of renewable sources like solar and wind to the grid, enabling efficient energy conversion and minimizing harmonic distortion [24, 25]. Additionally, these converters are finding applications in power factor correction and uninterruptible power supplies (UPS), where they contribute to improved energy quality and reliability [26].

Considering the advantages listed for this type of converter, the need to investigate their various usages in power networks are extremely felt. Thus, following the above discussion, this paper presents a novel exploration of NSCs, emphasizing their versatile applications and distinct advantages in modern power systems. By detailing the design, control strategies, and specific use cases such as Direct Torque Control (DTC) for induction motors, PV solar array operation, power factor improvement, fault ride-through in wind turbines, and electric vehicles, the paper highlights the unique ability of NSCs to enhance efficiency, flexibility, and performance across various power electronic applications. The novelty lies in the comprehensive analysis of NSCs' potential to minimize harmonic distortion, reduce component count, and achieve higher efficiency, all while maintaining cost-effectiveness. This multifaceted review not only consolidates existing knowledge but also identifies future research directions, underscoring NSCs pivotal role in advancing power conversion technologies. The main contributions of the paper are as follows:

*The paper provides an in-depth analysis of the nine-switch converter advantages, highlighting its cost-effectiveness, compact size, improved efficiency, enhanced reliability and application versatility. This analysis helps in understanding the practical benefits of NSCs over traditional converters and justifies their adoption in various power system applications.

* The paper introduces innovative configurations and control strategies for the nine-switch converter, optimizing its performance for different power systems applications. By presenting new circuit designs and advanced control algorithms, the paper contributes to the improvement of waveform quality, efficiency, and dynamic response, enhancing the overall functionality of the NSC in real-world scenarios.

* The paper explores and demonstrates the application of nine-switch converters in diverse power system scenarios, such as renewable energy integration, electric vehicle drives, and industrial motor drives.

The remainder of the paper can be organized as follows. Section 2 represents the general schematic of nine switch converters with its basic concepts. Different implementations of NSCs are discussed in section 3. Section 4 states the

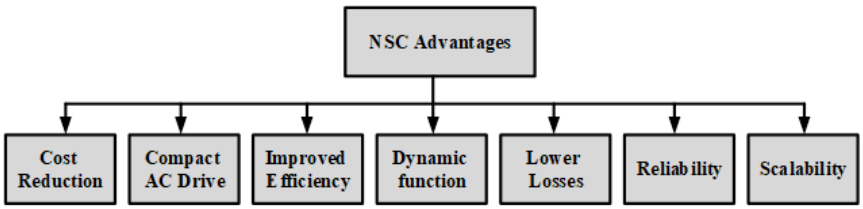

Figure 1. Key benefits of nine-switch converters.

future studies, and finally, conclusion is given in section 5.

2. Schematic of an NSC

A nine-switch converter (NSC) is constructed with three parallel branches, where each branch comprises a series connection of three power devices. The circuit arrangement is illustrated in Fig. 2. The NSC encompasses 8 distinct switching states within each leg, although certain states must be avoided to prevent abnormal operation of the converter. The remaining functional switching states are referred to as effective switching states, as they enable the proper functioning of the converter [27].

In a Nine-Switch Converter, the three-phase output voltages can be expressed as a function of the switching states of the nine switches and the input DC voltage. Each switch can be represented by a switching function $S_(i,j)$ where i represents the phase (A, B, C) and j represents the switch position (upper or lower).

$S_{(i,j)}$ = 1 When the upper switch is ON and the lower switch is OFF.

$S_{(i,j)}$ = 0 When the upper switch is OFF and the lower switch is ON.

According Fig. 2, the output phase voltages v_{oa}, v_{ob}, and v_{oc} can be derived from the switching functions and the DC bus voltage, E:

$$v_{oa} = \frac{E}{2}(S1H - S2H)$$
$$v_{ob} = \frac{E}{2}(S1M - S2M)$$
$$v_{oc} = \frac{E}{2}(S1L - S2L)$$

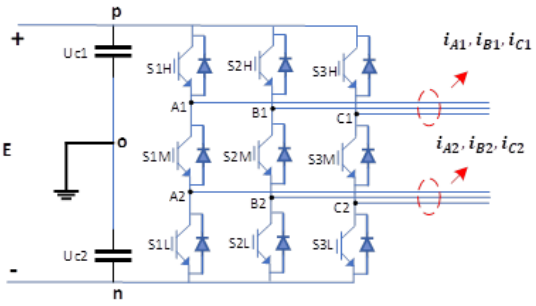

Figure 2. General topology of NSC.

Assuming balanced operation and resistive-inductive load R, L connected to the output, the current equations in the steady state can be expressed as:

$$E.(\frac{S1H - S2H}{2}) = i_A.R + L.\frac{di_A}{dt}$$
$$E.(\frac{S1M - S2M}{2}) = i_B.R + L.\frac{di_B}{dt}$$
$$E.(\frac{S1L - S2L}{2}) = i_C.R + L.\frac{di_C}{dt}$$

The state space model of the above equations described as follows:

$$\frac{d}{dt}\begin{bmatrix} i_A \\ i_B \\ i_C \end{bmatrix} = \begin{bmatrix} -\frac{R}{L} & 0 & 0 \\ 0 & -\frac{R}{L} & 0 \\ 0 & 0 & -\frac{R}{L} \end{bmatrix} \times \begin{bmatrix} i_A \\ i_B \\ i_C \end{bmatrix} + \begin{bmatrix} \frac{1}{L} & 0 & 0 \\ 0 & \frac{1}{L} & 0 \\ 0 & 0 & \frac{1}{L} \end{bmatrix} \times \begin{bmatrix} v_{oa} \\ v_{ob} \\ v_{oc} \end{bmatrix}$$

This model exhibits nonlinear behavior and varies over time. However, by applying the d-q transformation to this model with an angular frequency corresponding to the grid line frequency (ω), a time-invariant model can be derived. In this transformed model, the d-axis component of the supply phase voltage becomes zero.

$$\frac{d}{dt}\begin{bmatrix} i_d \\ i_q \end{bmatrix} = \begin{bmatrix} -\frac{R}{L} & \omega \\ \omega & -\frac{R}{L} \end{bmatrix} \times \begin{bmatrix} i_d \\ i_q \end{bmatrix} + \begin{bmatrix} \frac{1}{L} & 0 \\ 0 & \frac{1}{L} \end{bmatrix} \times \begin{bmatrix} v_d \\ v_q \end{bmatrix}$$

NSCs provide flexible control over the flow of electrical energy. They utilize nine switches, typically a combination of MOSFETs or IGBTs, to enable various operating modes. The control methods of nine-switch converters depend on the desired application and system requirements. Table 1 explores two major control strategies for this type of converter.

3. NSC applications

This section delves into the significant utilization of nine-switch converters within power systems and electric machines, aiming to offer researchers a comprehensive understanding and pave the way for the widespread adoption of these highly efficient converters.

3.1 Direct torque control of induction motors

The NSC is a new tool with dual output capabilities that enables the independent operation of two three-phase loads. In contrast, Direct Torque Control (DTC) represents a robust control scheme for AC motors, where careful selection of state vectors of a conventional voltage source inverter plays a crucial role. However, due to the distinctive operating principle of the NSC compared to the conventional voltage source inverter and the varying impact of active space vectors on motor torque and stator flux, [28] suggests the implementation of Direct Torque Control to efficiently drive two independent induction motors using the NSC. The objective is to minimize torque and stator flux ripples for both motors during operation.

In this study, the DTC control method is first described, and then the use of NSC in this control system is discussed. The DTC control scheme encompasses two distinct modes of operation: a) DTC torque mode, which directly controls the motor torque, and b) DTC speed mode, which controls the motor torque indirectly through the motor speed. In the direct DTC scheme, the inverter state vectors are carefully chosen to control both the stator flux and the electromagnetic torque. To ensure the proper functioning of the DTC control scheme, an accurate model of the induction motor is necessary. This is because the estimation of the stator

Table 1. Widely used control technique for nine-switch converters.

Control Strategy	Contributions
Space Vector Modulation (SVM)	-It allows for precise control of the output voltage or current by adjusting the duty cycles of the nine switches. -SVM calculates the reference voltage vectors and determines the appropriate switching states to generate the desired output waveform.
Pulse Width Modulation (PWM)	-It involves generating a high-frequency carrier waveform and comparing it with a reference signal. -By adjusting the width of the carrier pulses, the converter can regulate the output voltage or current.

flux and electromagnetic torque relies on the motor model. Consequently, the following equation can be formulated within this approach:

$$\vec{T} = \frac{3}{2}\frac{P}{2}\frac{L_m}{\sigma L_s L_r}\vec{\psi}_r \otimes \vec{\psi}_s \tag{1}$$

$$|\vec{T}_e| = \frac{3}{2}\frac{P}{2}\frac{L_m}{\sigma L_s L_r}|\psi_r||\psi_s|\sin\theta_{sr} \tag{2}$$

Where, ψ_s and ψ_r are the stator and rotor flux space vectors respectively. L_s , L_r and, L_m are stator inductance, rotor inductance and mutual inductance. P represents the number of poles. σ shows the leakage coefficient [28].

On the other hand, in the DTC speed mode control scheme, several parameters are measured and estimated for effective control. This includes the measurement of three-phase stator currents and stator voltages, as well as the estimation or measurement of motor speed using an encoder. The magnitude and angle of the stator flux are then estimated based on the obtained currents and voltages.

Now that the concept of DTC has been defined, to achieve independent control of the two loads, the NSC is designed to supply power to only one load at a time. When one load is being supplied, the phases of the second load are short-circuited through one of the DC rails. However, subsequent analytical investigations conducted by [29] revealed that the rates of increase and decrease in torque and stator flux values are not equal during successive switching:

$$\Delta T_e \uparrow = [P(\vec{\psi}_r \otimes \vec{v}_s) - Pw_r\vec{\psi}_r{}^{\circ}\vec{\psi}_s - R_m T_e]T_f/L_f \tag{3}$$

$$\Delta T_e \downarrow = [-Pw_r\vec{\psi}_r{}^{\circ}\vec{\psi}_s - R_m T_e]T_f/L_\sigma \tag{4}$$

Where T_f is the sampling period, $\otimes$ stands for vector product while $^{\circ}$ denotes the scalar product and $R_m = (L_r R_s + L_s R_r)/(L_m R_m)$; $L_\sigma = (L_r L_s - L_m^2)/L_m$.

Consequently, controlling the two motors in an alternating manner with a 50% duty cycle does not guarantee optimal outcomes. Instead, it can result in asymmetry and high ripples, compromising performance. Moreover, within the framework of the Direct Torque Control (DTC) scheme, it has been observed that the stator flux experiences significant ripples, particularly in the low-speed region.

To address the challenge of minimizing ripples in the electromagnetic torque and stator flux for both motors while achieving a comparatively higher switching frequency, the aforementioned findings are utilized as the foundation for the development of a novel control scheme. This control scheme is based on the algorithm outlined in Fig. 3. Its primary objective is to leverage the identified facts and principles to optimize the control process and attain improved performance in terms of torque and flux stability.

Considering the aforementioned reasons, the control scheme prioritizes the control of torque over the control of stator flux. In the event that one or both of the motors exhibit a

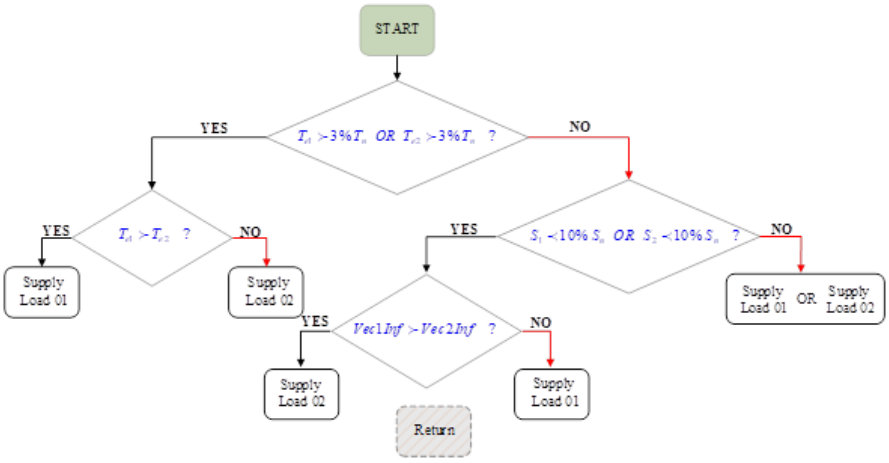

Figure 3. The Flow chart of the proposed algorithm [28].

significant torque error, the inverter will supply power to the load with the higher torque error. Conversely, if the torque errors for both loads are within an acceptable range, the selection process will favor the load whose vector has the least impact on changes in the stator flux, particularly when operating in the low-speed region. However, if the torque errors are acceptable and there is no specific focus on the stator flux, the selection between the two loads will be performed in an alternating manner.

3.2 PV solar array operation

Solar energy is an exceptional example of an inexhaustible resource, as it is derived from the vast amount of sunlight that reaches the Earth's surface. This abundant source of energy is available in practically unlimited quantities and is expected to continue for billions of years. Unlike fossil fuels, which are finite and subject to depletion, solar energy is constantly replenished by the sun, making it a sustainable and reliable option for meeting our energy needs [31, 32]. The conversion of solar energy into electrical energy involves various types of converters designed for specific applications. However, converters face challenges such as switching losses. In recent years, significant attention has been focused on reducing the number of switches in converter circuits. Nine switch converters represent a revolutionary advancement in this changing landscape, offering numerous advantages, including fewer switching devices, reduced switching losses, and improved power quality. In [30], a novel approach utilizing a photovoltaic solar array as the energy source, coupled with a nine switch converter to supply power to a load unit has been investigated. The voltage generated by the photovoltaic solar array is regulated using a dc-dc boost converter, which then feeds into the input of the nine-switch converter, ultimately providing power to the loads. The considered PV units of this study, including irradiation and temperature are as follows.

$$V_k = n_s \times \frac{S_i}{S_{iN}} \times T_C(T - T_N) + n \times (V_{max} - V_{min}) \times n_s \times \exp\left(\frac{S_i}{S_{iN}} \times \ln(V_{max} - V_{min})\right) \quad (5)$$

$$I_k = n_p \times \frac{S_i}{S_{iN}} \times (I_{Sc} + T_{Ci} + (T - T_N)) \quad (6)$$

where n_s and n_p are the total number of series and parallel-connected PV cells, S_i and S_{iN} denote solar irradiance and standard test condition irradiance, respectively. In addition, T_C is the temperature coefficient, V_{max} and V_{min} show the open circuit voltage at 1200 W/m^2 and 200 W/m^2 (298 K), respectively [30].
Equation (7) and (8) describe the correlation between the input and output voltage as well as current in the employed boost converter.

$$\frac{V_{output}}{V_{input}} = \frac{1}{1 - Duty\ cycle} \quad (7)$$

$$\frac{I_{input}}{I_{output}} = \frac{1}{1 - Duty\ cycle} \quad (8)$$

The block diagram of the proposed control strategy of PV cells comprises of PV unit, boost converter and NCS unit is illustrated in Fig. 4.

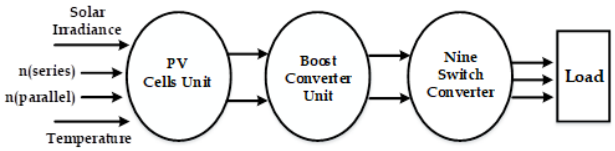

Figure 4. The proposed strategy of PV cells-NCS [30].

The switching vectors for the NSC vector control approach are shown in Table. 2. The findings indicate that the utilization and regulation of a solar PV cell can be achieved

Table 2. Switching Vectors in Control strategy of Nine Switch Converter [30].

Vector Number	1st Leg	2nd Leg	3rd Leg	Activation
1	1	0	0	Upper Switches
2	1	1	0	
3	0	1	0	
4	0	1	1	
5	0	0	1	
6	1	0	1	
7	-1	1	1	Lower Switches
8	-1	-1	1	
9	1	-1	1	
10	1	-1	-1	
11	1	1	-1	
12	-1	1	-1	
13	1	1	1	Zero Mode
14	0	0	0	
15	-1	1	-1	

successfully by employing a NSC instead of a 12-switch converter. This allows for independent operation when connected to different loads and the grid, showcasing the potential for effective control and implementation of solar energy resources.

3.3 Power factor improvement

Power electronic systems, such as rectifiers and inverters, are commonly used in various applications, including motor drives, renewable energy systems, and power supplies. The nine-switch converter is another power electronic converter topology that offers several advantages, including power factor improvement of a three-phase supply. These systems often employ DC link capacitors to store and release energy, providing smooth power flow and voltage regulation [33, 34].

By controlling the voltage across the DC link capacitor, it is possible to manipulate the power factor of the system. This is typically achieved through a control strategy called active power factor correction (APFC) [35]. APFC techniques actively adjust the voltage across the DC link capacitor to maintain a high-power factor and improve the overall efficiency of the system. In [36] to maintaining balance in the DC link capacitor and achieve power factor improvement a PID controller with injection the third harmonic is employed (Fig. 5). The capacitor's charging and discharging operations are contingent on the power transfer between the source and the load in both directions. In this control technique, active power can be transferred from the source to the load or vice versa by adjusting the angle δ, which represents the phase difference between the utility phase voltage and the rectifier modulating reference. Additionally, reactive power control can be achieved by modifying the amplitude v_r of the modulating reference. The modulation reference signals, incorporating a DC-offset, are expressed by Equation (9) and Equation (10).

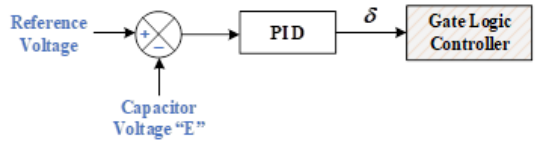

Figure 5. DC link capacitor controller [36].

$$v_r = m_r \sin[(2\pi f_r t) \pm \delta] + DC\ offset \tag{9}$$

$$v_i = m_i \sin[(2\pi f_r t) \pm \delta] - DC\ offset \tag{10}$$

Here, f_r refers to the reference frequency of the rectifier, and f_i represents the reference frequency of the inverter. The modulating references, denoted as v_r and v_i are utilized, where v_r signifies the rectifier reference, and v_i represents the inverter reference.

To enhance the utilization of the DC bus and improve power factor quality, the modulation references described by equations (9) and (10) incorporate the addition of a third harmonic component. The final modulating references for the NSC topology are derived from equations (11) and (12). It should be noted that by selecting the value of k as 1/6, which maximizes the DC bus utilization, the desired modulating references are obtained.

$$v_r^* = v_r + k \sin[3 \times (2\pi f_r t) \pm \delta] \tag{11}$$

$$v_i^* = v_i + k \sin[3 \times (2\pi f_i t) \pm \delta] \tag{12}$$

To illustrate the operation of the Gate Logic Controller depicted in Fig. 4, the three-phase, three-leg NSC converter shown in Fig. 1 is considered. In this configuration, specific switches are designated to function as diodes (S1H, S2H, S3H, S1M, S2M, and S3M) and others as inverters (S1M, S2M, S3M, S1L, S2L, and S3L). Notably, S1M, S2M, S3M serve dual purposes, operating as both inverters and diodes. The system presents three possible states where two switches per leg are turned ON while the third one is turned OFF. To provide a clearer understanding of this arrangement, Table. 3 is presented, illustrating the characteristics of a single leg in the 9-switch converter.

3.4 Wind turbine - fault ride through

The integration of wind energy systems into the power grid has led to the implementation of stricter regulations for connecting wind farms to the utility network. While a large number of recently produced and installed wind farms utilize Doubly-Fed Induction Generators (DFIG), a notable portion of the current wind turbines still rely on Fixed Speed Induction Generator based Wind Turbines (FSIG-WTs) [37–39].

The FSIG-WT operates by directly linking to the grid without any power electronics interface, necessitating the use of shunt capacitor banks to assist in fulfilling the generator's reactive power requirements. Consequently, the FSIG-WT exhibits inadequate voltage regulation and Fault Ride Through (FRT) capability. When a fault occurs, the terminal voltage drops, causing an imbalance between electrical and mechanical powers, which leads to an acceleration in generator speed and a substantial demand for reactive power. Additionally, network disturbances can trigger torsional modes in the WT-generator. Therefore, the integration of supplementary components becomes necessary to ensure voltage control and FRT compliance in accordance with the latest grid code mandates [40, 41].

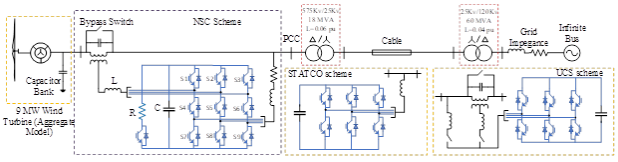

Figure 6. General diagram of system under study in [42].

To address the system dynamics and grid faults associated with FSIG-WT implementation, reference [42] employs a nine-switch converter (NSC) that enables both shunt and series compensation. This NSC serves to provide necessary adjustments and support in response to grid conditions and faults.

As demonstrated in Fig. 5, where the fault ride through structure for FSIG-WT is depicted, the NSC uses switches S1-S9 for its proper function. Specifically, switches S1-S6

Table 3. Switching states of a legs in the NSC for power quality application [36].

Switching state	S1H	S1M	S1L	V_{A1n}	V_{A2n}
1	ON	ON	OFF	E	E
2	OFF	ON	ON	0	0
3	ON	OFF	ON	E	0

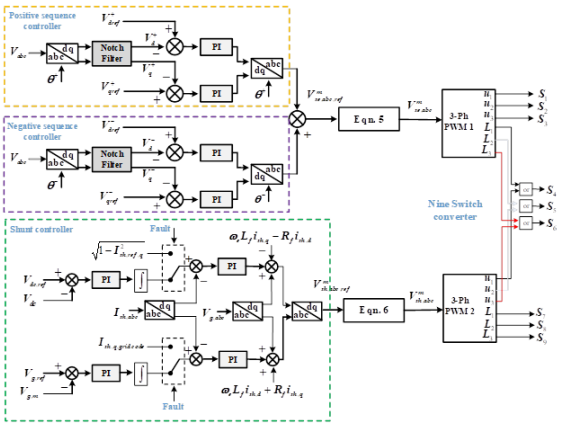

Figure 7. A comprehensive schematic of NSC control configuration for shunt-series compensation [42].

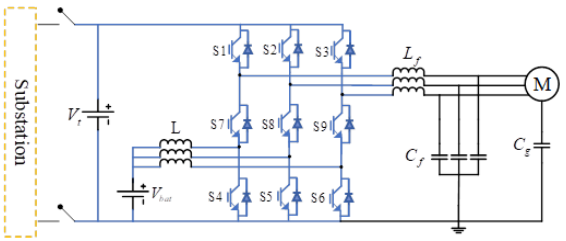

Figure 8. Schematic of multiport nine-switch converter [51].

are exploited for the series VSC, whereas switches S4-S9 are responsible for the shunt VSC. It is worth noting that switches S4, S5, and S6 are shared between the shunt and series converters. To mitigate the impact of switching harmonics, an appropriate LC filter is implemented. Furthermore, the shunt terminal is connected to the grid side of the series transformer, enabling the injection of reactive power during fault conditions. The Detailed control schematic of nine switch converter for shunt-series compensation is illustrated in Fig. 7.

From above figure, Equation (5) and (6) are stated as follows:

$$V_{shunt,abc} = V_{shunt,abc,ref} + \{(-1) - min(V_{shunt,abc,ref})\} \quad (13)$$

$$V_{series,abc} = V_{series,abc,ref} + \{1 - max(V_{series,abc,ref})\} \quad (14)$$

The effectiveness of the proposed scheme in improving the operation of Fault Ride-Through (FRT) and meeting the requirements outlined in the grid code has been substantiated through an extensive simulation study.

3.5 Electric transportation

In applications such as subways, suburban trains, high-speed trains, and electric tramways-collectively known as electrically powered rail transport-power electronics solutions featuring integrated and efficient converters with multiple functionalities are highly desirable. Among these, the nine-switch converter family stands out due to its ability to generate multiple output terminals with a reduced number of switches. In battery-powered tramways, the nine-switch converter presents a promising solution for achieving efficient, compact, and reliable power conversion. By utilizing this advanced converter topology, tramways can benefit from improved energy efficiency, a reduced component count, and enhanced operational flexibility. Consequently, [51] proposes a multiport converter solution based on the nine-switch converter topology that integrates multiple functionalities with a reduced switch count. This converter, which drives the power system of the electric tramway, is exclusively powered by a battery. Additionally, it incorporates a strategically connected passive filter that provides a low-impedance path for high-frequency currents, preventing leakage current circulation in the induction motor. Its phase-shift pulse-width modulation effectively reduces the high-frequency components of the current delivered by the battery.

The nine-switch converter proposed in the [51] offers significant benefits and key differences compared to the conventional structure, which typically involves traditional Voltage Source Inverters (VSIs). One of the primary advantages is the ability to enable bidirectional conversion between DC and AC, allowing control over both amplitude and frequency. This flexibility is essential for battery-powered tramways that require efficient switching between motoring and regenerative braking modes.

The nine-switch converter achieves its functionality with only nine switches, unlike conventional setups that generally require twelve switches. This reduction in the number of switches leads to lower costs, improved reliability, and a more compact design. Additionally, the proposed converter can generate two sets of three-phase outputs, essentially functioning as two separate VSI units with a single converter. This dual-output capability enhances operational flexibility and reduces the need for multiple converters. The scheme of multiport nine-switch converter presented by [51] is shown in the Fig. 8.

According to Fig. 8, when providing power to the load, the proposed topology functions in boost mode, channeling power from the second port to the first port. During regenerative braking, it shifts to buck mode, enabling the Energy Storage System (ESS) to absorb energy.

The system outlined in [51] utilizes a nine-switch multiport converter to drive a three-phase motor. This converter features two distinct energy processing units, referred to as the

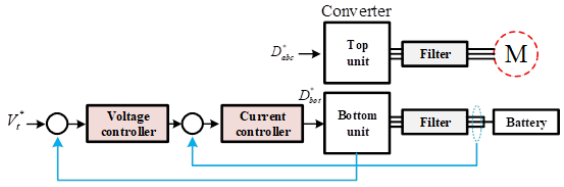

Figure 9. Comprehensive block diagram of the control system.

top and bottom units, which can be operated independently, as depicted in Fig. 9.

The top unit is dedicated to driving the three-phase motor, allowing for precise control over speed and torque to enhance motor performance. However, this study employs an open-loop control strategy, which models the steady-state behavior of the system while accounting for variations in load based on a typical electric tram load profile.

At last, it is worth mentioning that some research papers have conducted experimental setups on nine-switch converters. The experimental setups typically involve rigorous testing under diverse conditions to validate the theoretical models and to enhance the converters' efficiency, reliability, and performance. Table. 4 demonstrates the projects that have tested NSCs experimentally for different purposes.

4. Comparison and future prospectives

Table. 5 presents a fair comparison table between nine switch converters and conventional converters across various aspects.

As the electrification of transportation continues to accelerate and the demand for efficient energy management grows, nine switch converters are poised to play a crucial role. In addition to the special applications that NSCs have found in the field of electric ships [52] or charging and discharging batteries in electric vehicles [53], they can also be employed in uninterruptible power supplies (UPS). The bidirectional functionality of these converters makes them well-suited for UPS systems. On the other hand, NSCs would be able to integrate with HVDC grids to enhance power flow, improving fault handling, and increasing the scalability and reliability. These advantages contribute to the efficient transmission of electrical power, proposing a promising technology for the future development of HVDC networks.

5. Conclusion

In conclusion, this paper briefly reviews nine switch converters (NSCs), which represent a promising and versatile technology with a wide range of applications across multiple sectors. Their bidirectional power flow capability, enhanced fault handling, and modular design make them highly suitable for various power systems, including electric mobility, renewable energy integration, microgrids, industrial power systems, UPS, smart grids, and energy storage systems. Moreover, their utilization in HVDC grids offers significant advantages such as improved grid stability, efficient power control, seamless AC integration, and scalability. As the demand for efficient power flow control and energy management continues

Table 4. Summary of main experimental tests conducted on NSCs for various applications.

Reference [43]	Three-phase UPS application
Reference [44]	Carrier-based phase-shift space vector modulation
Reference [45]	Photovoltaic (PV) source of array
Reference [46]	Model predictive control approach of nine switch inverter-based drive systems
Reference [47]	PV grid-tied systems
Reference [48]	Direct model predictive control of nine switch inverter for dual-output mode operation
Reference [49]	Nine switch inverter to control two induction motors
Reference [50]	DFIG wind generation system

Table 5. Comparing different aspects of nine switch converters and conventional converters.

Aspect	Nine Switch Converters	Conventional Converters
Component Count	Reduced number of switches (9 in total), fewer passive components.	Higher number of switches, each converter stage requires its own set of switches and components.
Efficiency	Higher efficiency due to reduced switching losses and shared components.	Typically lower efficiency due to increased switching losses and multiple stages.
Cost	Lower cost due to fewer components and integrated design.	Higher cost due to the need for more components and separate converter stages.
Control Complexity	More complex control algorithms needed to manage shared switches and multiple outputs.	Simpler control due to independent stages but requires coordination between stages.
Size and Weight	More compact and lighter due to integrated design and fewer components.	Larger and heavier due to multiple stages and more components.
Thermal Management	Easier thermal management due to fewer heat-generating components.	More challenging due to multiple stages and higher heat generation.
Switching Frequency	Typically higher, allowing for smaller passive components.	Can vary widely, but generally lower switching frequencies in each stage.
Power Quality	Can offer improved power quality with appropriate control strategies.	Power quality depends on the design of each stage, typically requiring additional filtering.

to grow, the adaptable nature of nine switch converters positions them as a key contributor to the future of power electronics and grid systems.

Authors contributions
Authors have contributed equally in preparing and writing the manuscript.

Availability of data and materials
The authors declare that the data supporting the findings of this study are available within the paper.

Conflict of interests
The authors declare that they have no known competing financial interests or personal relationships that could have appeared to influence the work reported in this paper.

References

[1] F. Blaabjerg, K. Ma, and Y. Yang. "**Power electronics for renewable energy systems-status and trends**.". *CIPS 2014; 8th International Conference on Integrated Power Electronics Systems*, pages 1–11, 2014. URL https://ieeexplore.ieee.org/abstract/document/6776841.

[2] M. H. Mousavi, H. M. CheshmehBeigi, and M. Ahmadi. "**A DDSRF-based VSG control scheme in islanded microgrid under unbalanced load conditions**.". *Electrical Engineering*, 105(6):4321–4337, 2023.
DOI: https://doi.org/10.1007/s00202-023-01941-0.

[3] T. Dragičević, S. Vazquez, and P. Wheeler. "**Advanced control methods for power converters in DG systems and microgrids**.". *IEEE Transactions on Industrial Electronics*, 68(7):5847–5862, 2020.
DOI: https://doi.org/10.1109/TIE.2020.2994857.

[4] M. H. Mousavi and H. Moradi. "**Simultaneous compensation of distorted DC bus and AC side voltage using enhanced virtual synchronous generator in Islanded DC microgrid**.". *International Journal of Electronics*, 112(1):151–176, 2025.
DOI: https://doi.org/10.1080/00207217.2023.2278440.

[5] O. Krishan and S. Suhag. "**An updated review of energy storage systems: Classification and applications in distributed generation power systems incorporating renewable energy resources**.". *International Journal of Energy Research*, 43(12):6171–6210, 2019.
DOI: https://doi.org/10.1002/er.4285.

[6] D. Ronanki and S. S. Williamson. "**Modular multilevel converters for transportation electrification: Challenges and opportunities**.". *IEEE Transactions on Transportation Electrification*, 4(2):399–407, 2018.
DOI: https://doi.org/10.1109/TTE.2018.2792330.

[7] Z. Qin, P. C. Loh, and F. Blaabjerg. "**Application criteria for nine-switch power conversion systems with improved thermal performance**.". *IEEE Transactions on Power Electronics*, 30(8): 4608–4620, 2014.
DOI: https://doi.org/10.1109/TPEL.2014.2360629.

[8] A. Choudhury, S. Pati, R. Sharma, and S. K. Kar. "**Real-Time Implementation of Electric Spring Using a Nine Switch Converter Topology for Combined Power Control in a Hybrid Microgrid System**.". *Arabian Journal for Science and Engineering*, pages 1–16, 2023.
DOI: https://doi.org/10.1007/s13369-023-07846-1.

[9] A. A. Dongre, J. P. Mishra, and R. K. Majji. "**Nine Switch Multifunctional Converter Configuration for Integrating Dynamic Voltage Restorer and Solar Photovoltaic**.". *IEEE*, pages 1–6, 2022.
DOI: https://doi.org/10.1109/ICICCSP53532.2022.9862373.

[10] K. Ali, P. Das, and S. K. Panda. "**A special application criterion of the nine-switch converter with reduced conduction loss**.". *IEEE Transactions on Industrial Electronics*, 65(4):2853–2862, 2017.
DOI: https://doi.org/10.1109/TIE.2017.2748044.

[11] S. M. D. Dehnavi, M. Mohamadian, A. Yazdian, and F. Ashrafzadeh. "**Space vectors modulation for nine-switch converters**.". *IEEE Transactions on Power Electronics*, 25(6):1488–1496, 2009.
DOI: https://doi.org/10.1109/TPEL.2009.2037001.

[12] J. Guo. "**Research on simplified SVPWM strategy for nine-switch converter**.". *Journal of Power Electronics*, 20(6):1386–1394, 2020.
DOI: https://doi.org/10.1007/s43236-020-00124-5.

[13] E. Can. "**Fault determination and analysis of complex switching structure at multilevel inverter**.". *Tehnički vjesnik*, 26(2):398–404, 2019.
DOI: https://doi.org/10.17559/TV-20180417194701.

[14] J. Zhang, L. Li, and D. G. Dorrell. "**Control and applications of direct matrix converters: A review**.". *Chinese Journal of Electrical Engineering*, 4(2):18–27, 2018.
DOI: https://doi.org/10.23919/CJEE.2018.8409346.

[15] P. C. Loh, A. S. Bahman, Z. Qin, and F. Blaabjerg. "**Evaluation of switch currents in nine-switch energy conversion systems**.". *IEEE*, pages 755–760, 2013.
DOI: https://doi.org/10.1109/IECON.2013.6699229.

[16] R. Vargas, U. Ammann, and J. Rodriguez. "**Predictive approach to increase efficiency and reduce switching losses on matrix converters**.". *IEEE Transactions on Power Electronics*, 24(4):894–902, 2009.
DOI: https://doi.org/10.1109/TPEL.2008.2011907.

[17] G. Villar-Pique, H. J. Bergveld, and E. Alarcon. "**Survey and benchmark of fully integrated switching power converters: Switched-capacitor versus inductive approach**.". *IEEE Transactions on power electronics*, 28(9):4156–4167, 2013.
DOI: https://doi.org/10.1109/TPEL.2013.2242094.

[18] E. C. Dos Santos, C. B. Jacobina, and O. I. Da Silva. "**Six-phase machine drive system with nine-switch converter**.". *IEEE*, pages 4204–4209, 2011.
DOI: https://doi.org/10.1109/IECON.2011.6119776.

[19] K. C. Wu. "**Switch-mode power converters: Design and analysis**.". *Elsevier*, 2005.
DOI: https://doi.org/10.1016/B978-0-12-088795-8.X5000-4.

[20] L. Pan, J. Zhang, J. Zhang, Y. Pang, B. Wang, K. Wang, and D. Xu. "**A novel space-vector modulation method for nine-switch converter**.". *IEEE Transactions on Power Electronics*, 35(2):1789–1804, 2019.
DOI: https://doi.org/10.1109/TPEL.2019.2923124.

[21] A. Abdelhakim, T. B. Soeiro, M. Stecca, and F. Canales. "**Multiport hybrid converter for electrified transportation systems**.". *IEEE Transactions on Industrial Electronics*, 70(7):6819–6829, 2022.
DOI: https://doi.org/10.1109/TIE.2022.3199857.

[22] P. Wang, H. Xu, and L. Yuan. "**Research on cascaded multilevel converters for dual motor drive systems based on a nine-switch converter**.". *IET Electric Power Applications*, 2024.
DOI: https://doi.org/10.1049/elp2.12441.

[23] E. Can and U. Kilic. "**A new high-frequency multilevel inverter effecting cables weight and energy efficiency of aircraft**.". *Aircraft Engineering and Aerospace Technology*, 96(3):458–464, 2024.
DOI: https://doi.org/10.1108/AEAT-06-2023-0158.

[24] V. F. Pires, D. M. Sousa, and J. F. Martins. "**Three-phase nine switch inverter for a grid-connected photovoltaic system**.". *IEEE*, pages 1078–1083, 2013.
DOI: https://doi.org/10.1109/ICRERA.2013.6749913.

[25] E. Can. "**Torques and the speed vibrations reducing and optimization of asynchronous motor with ECCA-PID controlling in power system**.". *Sādhanā*, 49(2):126, 2024.
DOI: https://doi.org/10.1007/s12046-024-02491-2.

[26] C. N. Jibhakate, M. A. Chaudhari, and M. M. Renge. "**Nine-switch controlled induction motor drive with unity and leading power factor**.". *IEEE*, pages 1–6, 2017.
DOI: https://doi.org/10.1109/ICECCT.2017.8117994.

[27] D. Liu, X. Zhang, L. Pan, and A. Li. "**Modelling and Control of Nine-Switch Converter-Based DFIG Wind Power System**.". *Journal of Electrical Engineering & Technology*, 15:2587–2599, 2020.
DOI: https://doi.org/10.1007/s42835-020-00506-6.

[28] D. Abdelghani and A. Boumediène. "**Direct torque control of two induction motors using the nine-switch inverter**.". *International Journal of Power Electronics and Drive Systems (IJPEDS)*, 9(4): 1552–1564, 2018.
DOI: https://doi.org/10.11591/ijpeds.v9.i4.pp1552-1564.

[29] G. A. Munoz-Hernandez, G. Mino-Aguilar, J. F. Guerrero-Castellanos, and E. Peralta-Sanchez. "**Fractional order PI-based control applied to the traction system of an electric vehicle (EV)**.". *Applied Sciences*, 10(1):364, 2020.
DOI: https://doi.org/10.3390/app10010364.

[30] R. Kumar and A. Agarwal. "**Implementation of Nine-Switch converter to PV solar array operating with different loads**.". *Materials Today: Proceedings*, 51:670–676, 2022.
DOI: https://doi.org/10.1016/j.matpr.2021.06.160.

[31] R. Rostami, S. M. Khoshnava, H. Lamit, D. Streimikiene, and A. Mardani. "**An overview of Afghanistan's trends toward renewable and sustainable energies**.". *Renewable and Sustainable Energy Reviews*, 76:1440–1464, 2017.
DOI: https://doi.org/10.1016/j.rser.2016.11.172.

[32] S. Algarni, V. Tirth, T. Alqahtani, S. Alshehery, and P. Kshirsagar. "**Contribution of renewable energy sources to the environmental impacts and economic benefits for sustainable development**.". *Sustainable Energy Technologies and Assessments*, 56:103098, 2023.
DOI: https://doi.org/10.1016/j.seta.2023.103098.

[33] M. A. Chaudhari, H. M. Suryawanshi, and M. M. Renge. "**A three-phase unity power factor front-end rectifier for AC motor drive**.". *IET Power Electronics*, 5(1):1–10, 2012.
DOI: https://doi.org/10.1049/iet-pel.2011.0029.

[34] M. Ahmadi, P. Sharafi, M. H. Mousavi, and F. Veysi. "**Power quality improvement in microgrids using statcom under unbalanced voltage conditions**.". *International Journal of Engineering*, 34(6): 1455–1467, 2021.
DOI: https://doi.org/10.5829/ije.2021.34.06c.09.

[35] A. Sun and L. Niu. "**Input-Series-Output-Parallel LLC Resonant Converter with Input Power Factor Correction for AGV Chargers**.". *The Proceedings of the 9th Frontier Academic Forum of Electrical Engineering*, I:309–317, 2021.
DOI: https://doi.org/10.1007/978-981-33-6606-0-29.

[36] C. N. Jibhakate, M. A. Chaudhari, and M. M. Renge. "**Power factor improvement using nine switch AC-DC-AC converter**.". *IEEE*, pages 1–4, 2016.
DOI: https://doi.org/10.1109/ICPES.2016.7584169.

[37] F. Blaabjerg and K. Ma. "**Future on power electronics for wind turbine systems**.". *IEEE Journal of emerging and selected topics in power electronics*, 1(3):139–152, 2013.
DOI: https://doi.org/10.1109/JESTPE.2013.2275978.

[38] L. Holdsworth, J. B. Ekanayake, and N. Jenkins. "**Power system frequency response from fixed speed and doubly fed induction generator-based wind turbines**.". *Wind Energy: An International Journal for Progress and Applications in Wind Power Conversion Technology*, 7(1):21–35, 2005.
DOI: https://doi.org/10.1002/we.105.

[39] A. Moghadasi and A. Islam. "**Enhancing LVRT capability of FSIG wind turbine using current source UPQC based on resistive SFCL**.". *IEEE*, pages 1–5, 2014.
DOI: https://doi.org/10.1109/TDC.2014.6863374.

[40] L. Meegahapola, M. Datta, I. Nutkani, and J. Conroy. "**Role of fault ride-through strategies for power grids with 100% power electronic-interfaced distributed renewable energy resources**.". *Wiley Interdisciplinary Reviews: Energy and Environment*, 7(4):e292, 2018.
DOI: https://doi.org/10.1002/wene.292.

[41] A. R. A. Jerin, P. Kaliannan, and U. Subramaniam. "**Testing of low-voltage ride through capability compliance of wind turbines-a review**.". *International Journal of Ambient Energy*, 39(8):891–897, 2018.
DOI: https://doi.org/10.1080/01430750.2017.1340337.

[42] A. Kirakosyan, M. S. El Moursi, P. Kanjiya, and V. Khadkikar. "**A nine-switch converter-based fault ride through topology for wind turbine applications**.". *IEEE Transactions on Power Delivery*, 31 (4):1757–1766, 2016.
DOI: https://doi.org/10.1109/TPWRD.2016.2547942.

[43] C. Liu, B. Wu, N. Zargari, D. Xu, and J. Wang. "**Novel nine-switch PWM rectifier-inverter topology for three-phase UPS applications**.". *EPE Journal*, 19(2):36–44, 2009.
DOI: https://doi.org/10.1080/09398368.2009.11463715.

[44] N. Jarutus and Y. Kumsuwan. "**A carrier-based phase-shift space vector modulation strategy for a nine-switch inverter**.". *IEEE Transactions on Power Electronics*, 32(5):3425–3441, 2016.
DOI: https://doi.org/10.1109/TPEL.2016.2587811.

[45] P. K. Nalli, K. S. Kadali, R. Bhukya, V. Rajeswari, and D. P. Garapati. "**Experimental Validation for A Nine-Switched 3-phase Multilevel Inverter (MLI) With a Photovoltaic (PV) Source of Array**.". *Journal of Physics: Conference Series.IOP Publishing*, 2089(1):012021, 2021.
DOI: https://doi.org/10.1088/1742-6596/2089/1/012021.

[46] O. Gulbudak and M. Gokdag. "**Finite control set model predictive control approach of nine switch inverter-based drive systems: Design, analysis, and validation**.". *ISA transactions*, 110:283–304, 2021.
DOI: https://doi.org/10.1016/j.isatra.2020.10.037.

[47] L. Jiang, Y. Chen, F. Dai, K. Liu, X. Chen, and X. He. "**A nine-switch inverter with reduced leakage current for PV grid-tied systems using model-free predictive current control**.". *Energy Reports*, 9:396–405, 2023.
DOI: https://doi.org/10.1016/j.egyr.2023.05.170.

[48] O. Gulbudak and M. Gokdag. "**Asymmetrical multi-step direct model predictive control of nine-switch inverter for dual-output mode operation**.". *IEEE Access*, 7:164720–164733, 2019.
DOI: https://doi.org/10.1109/ACCESS.2019.2953141.

[49] O. Gulbudak and M. Gokdag. "**Dual-hysteresis band control of nine-switch inverter to control two induction motors**.". *IEEE Transactions on Energy Conversion*, 37(2):788–799, 2021.
DOI: https://doi.org/10.1109/TEC.2021.3131385.

[50] K. Wang, J. Zhang, Y. Pang, D. Xu, and L. Pan. "**Modeling of nine-switch-converter based on virtual leg and its application in DFIG wind generation system**.". *IEEE Transactions on Power Electronics*, 35(7):7674–7688, 2019.
DOI: https://doi.org/10.1109/TPEL.2019.2958425.

[51] A. D. Almeida, F. Bradaschia, C. Rech, C. A. Caldeira, R. C. Neto, and G. M. Azevedo. "**Nine-Switch Multiport Converter Applied to Battery-Powered Tramway with Reduced Leakage Current**.". *Energies*, 17(6):1434, 2024.
DOI: https://doi.org/10.3390/en17061434.

[52] C. A. Reusser and H. Young. "**Nine-switch converter application on electric ship propulsion—A redundancy approach**.". *IEEE*, pages 1–7, 2016.
DOI: https://doi.org/10.1109/ESARS-ITEC.2016.7841389.

[53] M. S. Diab, A. A. Elserougi, A. S. Abdel-Khalik, A. M. Massoud, and S. Ahmed. "**A nine-switch-converter-based integrated motor drive and battery charger system for EVs using symmetrical six-phase machines**.". *IEEE Transactions on Industrial Electronics*, 63(9):5326–5335, 2016.
DOI: https://doi.org/10.1109/TIE.2016.2555295.